TOWARDS PASSIVE UNLABELED CELL SORTING IN A MICROFLUIDIC FLOW CHAMBER

A Thesis
Presented to
The Academic Faculty

by

Nicholas Frohberg

In Partial Fulfillment
of the Requirements for the Degree
Bachelor of Science for the Research Option in the
School of Biomedical Engineering

Georgia Institute of Technology
May 2018

TOWARDS PASSIVE UNLABELED CELL SORTING IN A MICROFLUIDIC FLOW CHAMBER

Approved by:

Dr. [Advisor Name], Advisor
School of [Whatever Engineering]
Georgia Institute of Technology

Dr. [Committee Member2]
School of [Whatever Engineering]
Georgia Institute of Technology

Dr. [Committee Member3]
School of [Whatever Science]
Georgia Institute of Technology

Date Approved: [Date Approved by Committee]

ACKNOWLEDGEMENTS

I wish to thank everyone in the Qiu Lab at Georgia Tech, especially principal investigator Dr. Peng Qiu, for providing me the opportunity to conduct this research as well as providing their support, assistance, and mentorship throughout my time working in the lab.

TABLE OF CONTENTS

LIST OF FIGURES

LIST OF SYMBOLS AND ABBREVIATIONS

FACS	Fluorescence activated cell-sorting
MACS	Magnetic activated cell-sorting
FEM	Finite element modelling
CFD	Computational fluid dynamics
CAD	Computer aided design
UI	User interface

SUMMARY

Cell separation is utilized for a variety of purposes in biomedicine, including clinical diagnosis, or batch purification or rare cell isolation within a research laboratory setting. The currently used methods for cell separation are mostly limited to fluorescent or magnetic activated cell sorting, or density-gradient methods. These methods have clear weaknesses; the former two have high monetary cost, and the requirement for tags can delay project completion by months, while density-gradient methods have poor accuracy. This work discusses a label-free passive method for sorting cells, through mechanical forces created by flow in a microfluidic chamber. This project aims to mathematically model the ways that a particular set of modifiable flow chamber parameters will influence the trajectory of cells with differing physical parameters. Water velocity within the device was modeled through the use of the finite element method and computational fluid dynamics. An analysis is performed on what the flow field inside this device looks like and how this can be manipulated for cell sorting. Initial observation shows that large, stiff, and weakly viscous cells will move upwards. This research and model could make it possible to successfully use this microfluidic flow chamber design to sort cell groups which had not previously been researched in this device.

CHAPTER 1

INTRODUCTION

Cell sorting is a useful and commonly practiced laboratory procedure which is utilized to purify a mixed batch of cells, or isolate a desired cell type for the purpose of quantification, experimentation, or diagnosis. Among the most frequently used cell sorting techniques are fluorescence-activated cell sorting (FACS) and magnetic-activated cell sorting (MACS) (1). These two sorting techniques are renowned for the high purity and precision of their sorting. However, these techniques both require the application of antibodies that are specialized for the chemical structure of the cells, which can cost thousands of dollars and take months to prepare (2). These shortcomings of the predominant methods of cell sorting call for research into more affordable techniques. Recently, there has been an increased interest in using microfluidic flow chambers for the purpose of cell sorting and disease diagnosis (3). Microfluidic flow chambers are a novel technology which exploit the differences in particles' physical properties for the purpose of particle sorting. Based on mechanical properties such as mass, size, elasticity, and viscosity, different particles will follow different trajectories when subjected to a complex flow-environment (4). One goal of a microfluidic flow chamber is to create a flow environment such that an input batch of different particle types will be carried to different outlets, where each outlet is positioned such that only one particle-type should reach it and flow through it (4). Since this flow environment will need to be custom-made based on what particle types are present in the input batch of particles, in order for the technology to be effective across many different particle types one will need an advanced

understanding of how a particle's trajectory is related to its mechanical properties and the flow field it is in.

Through trial and error, researchers have previously created flow chambers to sort a known treated and softened cell-type from its healthy counterpart (5) (6). Considering the nearly endless possible combinations of healthy and diseased cell-types that can be input to a flow chamber, there is a need for a predictive model that bypasses trial and error methodology. To develop such a model, several requisite tasks have been completed. It is necessary to both develop a program that can track cells as they move through the flow chamber, as well as to create a program which can simulate the flow of water through a custom-made chamber. We previously created the program that tracks cells, and this paper will explain the flow simulation (7).

To explain the observed cellular behavior, it is necessary to have a model for the flow of water through the chamber. Ultimately, it is the velocity of the water that results in the observed movement of the cells. In order to create a model for the velocity of water in a device, the finite element model (FEM) was applied to solve the Navier-Stokes equations for incompressible laminar flow across the geometry of our device. Once the fluid velocity is mapped to the flow chamber, a model can be constructed to explain the relation between the geometry of the device, and the trajectory of particular cell types. The application of this model will allow for microfluidic flow chambers to be custom-made in a manner that maximizes lateral displacement of cells, increasing cell batch purification, and making this microfluidic technique an increasingly viable alternative to the ubiquitous techniques of FACS and MACS.

CHAPTER 2

LITERATURE REVIEW

Microfluidic based cell sorting has the potential to allow for cheaper, simpler, and more convenient sorting and enrichment of cell types than the methodologies that are currently in practice (2). This technology is similar to previously established and marketed technologies which allow for DNA sorting and quantification, by subjecting the molecules to a magnetic field as they travel through a flow chamber (3). Cell sorting is a more complicated task, due to their reduced response to magnetic stimuli, as well as the more complex nature of the cell making a chemical-based sorting method such as those seen in many lab-on-a-chip devices to be infeasible (2). Due to the complexity of the task, there are many different approaches for microfluidic cell sorting devices. These methods are all imperfect and contain at least one weakness, such as low throughput, required labelling, high cost, or that sorting will only be achieved under limited and specific circumstances.

The most frequently used cell sorting methods used in current practice are FACS and MACS. These are high throughput and potentially precise sorting methods, which require a label (usually multiple) that is expected to be expressed in varying levels across the cell types that are to be sorted. These labels are often expensive, may take months to prepare, and may not be sufficient for sorting cell types, especially if a low concentration of the cell type is used (1). Since the labels attach to a specific chemical receptor on a

cell, the only property the cells are sorted by is its chemical markers. Many of the current alternative approaches are label free and sort by physical properties.

The most common physical property that can be used for cell sorting is cell volume. This can be exploited on a mechanical basis, or through the use of electrokinetics. Larger cells will carry a more negative charge, which will result in them being more responsive to an electromagnetic field; this can be used to laterally separate large and small cells in a microfluidic chamber (8). Unfortunately, different cell types often have similar sizes; if these are to be sorted through electrokinetics, it is still necessary to attach a charge-carrying label to these cells (8).

Mechanical approaches to cell sorting involve the construction of flow environments which alternate between steady and turbulent. Larger cells contain more inertia, and will be resistant to a change in direction when subject to the turbulent flow pattern (2). The result is that larger cells will be displaced less than smaller cells. This approach does not offer any way to separate cells that are the same size. Another approach is to have the cells flow through a tight space which contains a pressure sensor, which will measure the change in ionization as the cell compresses to fit through the space (6). This approach makes a measurement of the cell's stiffness, which is different between different cell types, and can even be used to determine if a cell of a known cell type is diseased. The drawback to this method is that it does not sort based on size, so it cannot distinguish between different cell types that require the same amount of energy to compress.

Our proposed technology is label free, and sort based on cell size, cell stiffness, and cell viscosity. To achieve this, we have constructed a device which has sections

where flow is in alternating directions, in addition to “tight” gaps which will force the cells into compression and sort based on their state of compression (4). With this combination of properties that can be utilized for cell sorting, and due to this being a label-free sorting method, we will be able to cost-effectively sort a large variety of cell types that have similar morphological characteristics. Compared to FACS and mass spectrometry, our device will additionally be able to discriminate between diseased cells and healthy cells, which may not present any notable chemical differences. This would allow for new ways to categorize disease states, which may lead to the administration of more specific treatments that corresponds to the individual’s disease state.

CHAPTER 3

FLUID MODELLING

The flow of the water must be understood, before a model for the flow of the cells can be created. Fluid modelling is already a well-developed field with many available tools and applications. For this project, the device was modeled as incompressible laminar flow. The task was completed through the use of Gmsh, a free meshing software, in conjunction with OpenFOAM, a free opensource flow and field equation solver (9) (10). Results were viewed and analyzed in ParaView, an opensource and free data visualization and analyzation tool (11).

Mesh Creation:

Gmsh was used for mesh creation. A mesh is a grid-like structure that details the discrete number of points that are to be used to model a particular geometry. Defining a finite number of elements, as is done in FEM, is a necessary task for many computational fluid dynamics (CFD) techniques which utilize discrete and iterative algorithms. Before Gmsh can create a mesh across the volume of the device, the boundaries of the device must be geometrically defined. The bounding walls of the device can be defined in a .geo file. In a .geo file, simpler elementary elements such as lines can be combined into higher dimensional geometry such as polygons. A set of polygons that completely bound an area can be defined as a volume. Once a volume has been defined, Gmsh can be used to create the mesh. Before the mesh is created though, there are several mesh parameters that must be changed.

Decreasing the distance between each point in a mesh will lead to more accurate and detailed results but will also increase the computational time. The default element size setting in Gmsh is far too large, and will result in very poor characterization of flow in the small regions that are between ridges. For this project, the element size factor was reduced to 0.1 or 0.08. After selecting the element size, it was important to increase the number of smoothing steps beyond 1. After these parameters are selected, a mesh was created through the mesh->3D option. After this mesh was created, the optimize 3D command was selected. Both the optimization and smoothing options act to increase the uniformity of the mesh, which has been generated in a non-uniform manner. Generally, mesh cells are higher quality if they are less skewed, which is to say that mesh cells should be made to have similar length sides (12). After the mesh was created, it was exported for use in OpenFOAM. An example of this mesh can be seen in Figure 1.

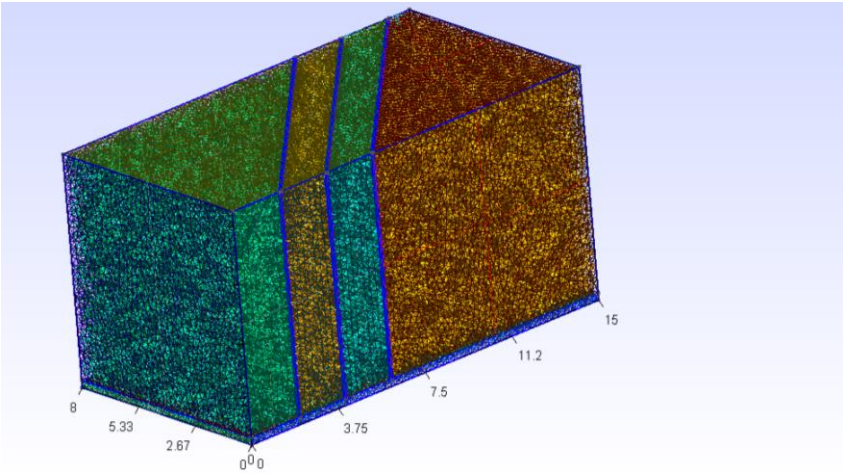

Figure 1. Microfluidic Flow Chamber Mesh. The mesh constructed from Gmsh. Each unique color represents a different surface. Blue represents regions that water cannot flow through. This device contains 3 ridges.

Flow Field Solver

Once the mesh has been created, and the inlet and outlet have been labeled, various characteristics of the flow scenario must be defined with OpenFOAM. For this project, a system dictionary and set of initial conditions files were created that will work for any mesh that was created based on the previously described methodology for our device. The initial conditions include that the inlet has a flow velocity of 0.1 in the x direction and a positive pressure. This particular velocity was identified to result in laminar, non-turbulent flow. The outlet acts as a pressure sink, which ensures that flow will head from the inlet to the outlet. All other surfaces are defined as solid walls which never act as pressure or velocity nodes or sinks. In the system dictionary file, the simulation is set to solve in steps of 0.005 seconds, and to stop running when 5 seconds have been simulated. During this time, the flow develops into its final steady state. Increasing the timestep will reduce the accuracy of the simulation. In this study, these parameters were successfully used to simulate the flow inside of the device. The primary way that the simulation could have failed is if the Courant number, which is equal to the velocity multiplied by the time step and divided by the length interval, becomes too large. A larger courant number tends to signify that the simulation will be less accurate (13).

After the flow field was calculated, the results were viewed in ParaView, a free 3D viewing software. An image of the y velocity at z = 0.025, halfway between the floor and the bottom of each ridge, can be seen in figure 3. Additionally, data was exported from ParaView as a .csv file, which contains an ordered list of the X, Y, Z coordinates, and the U, V, W velocities throughout the flow field. This data was then analyzed in MATLAB, and a proof-of-concept simulation of cell trajectory was performed. This

proof-of-concept simulation demonstrates that the flow will push a particle along a trajectory that resembles what has been observed for soft cells from real life experimentation (figure 4) (4).

Automated Geometry Creation

The previous simulated device was constructed manually, which was a time-consuming process. Although Gmsh, an open-source 3D finite-element-modelling (FEM) tool, simplifies geometry creation with a comprehensive computer aided design (CAD) user interface (UI), this process still requires an extensive number of operations. This manual process involved defining the walls of the device point by point, then line by line, and finally polygon by polygon. For a simple device, this amounted to 90 definitions that needed to be created. In order to expediate this process in the future, a MATLAB function was created that can automate the construction of the device, according to some specified parameters.

The MATLAB function accepts the following user-specified parameters: number of ridges, ridge angle, distance between each ridge, the width of each ridge, and the distance between the ridge and the floor of the device. The length of the device is automatically adjusted based on the input parameters. Additionally, there will be a length of 0.5 between the inlet and the first ridge, as well as a distance of 0.5 between the outlet and the last ridge. Finally, the appropriate surfaces are identified as the inlet and the outlet.

The MATLAB function will perform the previously mentioned operations, such that a device is created according to the user specified parameters. First, the length of the overall device is calculated with the following equation:

Length = distanceBetweenFirstRidge + distanceBetweenLastRidge + deviceWidth * tan(-ridgeAngle) + ridgeWidth * nRidges + ridgeSeperation * (nRidges-1)

In the current implementation, it is assumed that the distance between the first ridge and the inlet, as well as the last ridge and the outlet, are both 0.5. It is additionally assumed that the device width is 1.0. Perhaps the only term here that needs explanation is deviceWidth * tan(-ridgeAngle). This term is relating the width of the device and the angle of the device to the horizontal spread of a single ridge. The wider the device, or the greater the magnitude of the ridge angle, the more horizontal space it will occupy. A schematic of this can be seen in figure 2. It is worth noting that ridgeWidth is defined as the width along the x direction, rather than the minimum one-dimensional distance required to pass through the ridge. The difference between these two concepts becomes drastic as ridgeAngle approaches -pi/2.

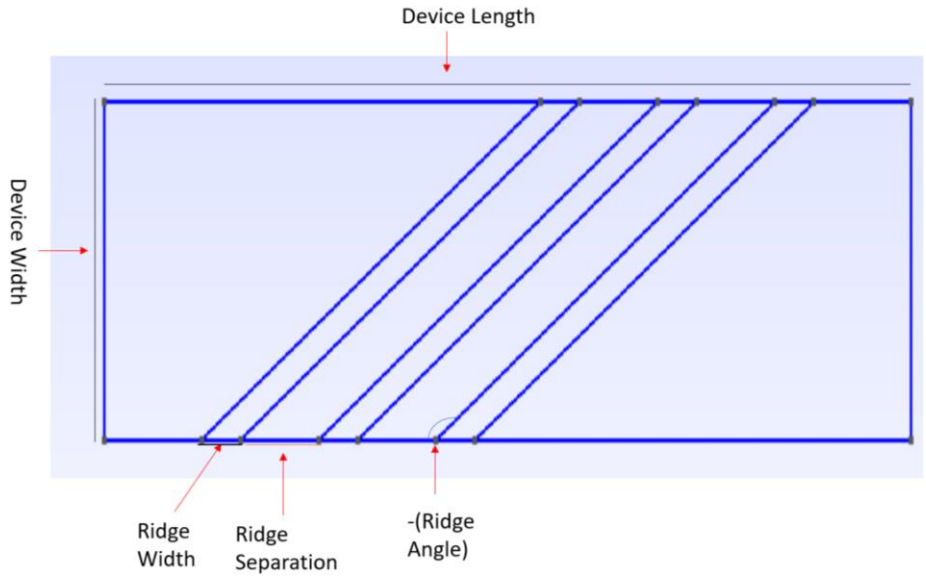

Figure 2. Device dimensions. The resulting .geo file as seen in Gmsh, with the various dimensions labeled. Y dimension is vertical, and X dimension is horizontal.

CHAPTER 4

RESULTS

ParaView was used to view the velocity field obtained from OpenFOAM, as can be seen in Figure 3. After the velocity data was imported, a slice-view was performed normal to the Z axis, at Z = 0.025, and at Z = 0.10. The value Z = 0.025 was selected, because this is halfway between the floor of the device and the ridges which the cells must flow underneath. Since the gap beneath the ridge is designed to be smaller than the cell, the cell will occupy almost all of the gap from Z = 0.0 to Z = 0.05. For this reason, it makes sense to check the flow at a plane between these two planes. The value Z = 0.10 was selected as a relatively low height that cells can possibly rise to in-between each ridge. The Y velocity is being visualized, as the goal of this device is to sort cells based on different displacement along the Y axis. In 3.A, it can be seen that the flow in the ridge section is always in the negative y direction, whereas in 3.B, the flow in the ridge section is always in the positive y direction. Additionally, it is known that flow is always from left to right in this device.

3.A

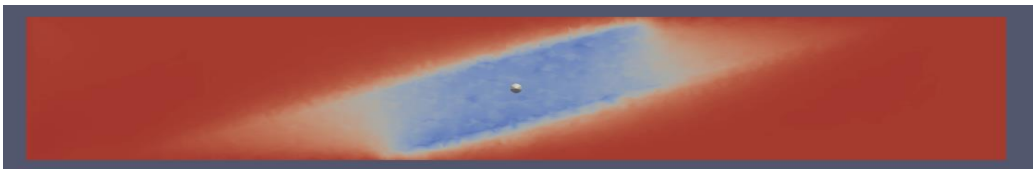

3.B

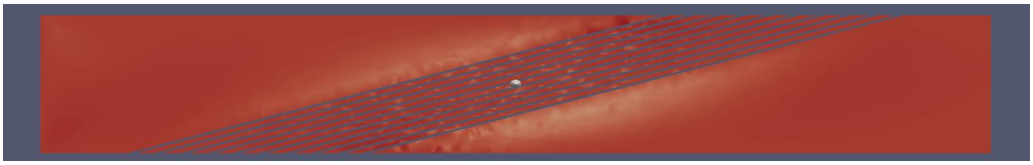

3.C

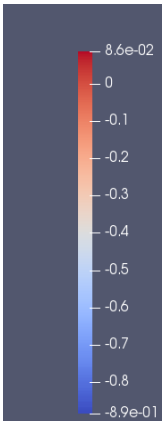

Figure 3. ParaView Visualisation of Y Velocity. (3.A.) Y Velocity at Z = 0.025 . (3.B.) Y velocity at Z = 0.1 Y dimension is vertical, and X dimension is horizontal. The white is the center of the device. (3.C). Color legend for Y velocity.

A proof-of-concept simulation of particles flowing through the device was created in MATLAB (figure 3). This simulation was built from data obtained from a .csv file that contained the velocity field data of our simulated device. In this simulation, the accelerations of the particle are determined based on the calculated water velocity at the particle's current position. The position of the particle is iteratively updated by an amount corresponding to its current velocity. The particle's acceleration in the z direction was modeled separately in two instances, to demonstrate that the z position of a particle is critical in determining its trajectory. The particle that had a z acceleration approximately 1.5 times larger would be displaced in the positive y direction in-between each ridge, whereas the particle with lesser z acceleration would be displaced in the negative y direction in-between each ridge, as seen in figure.

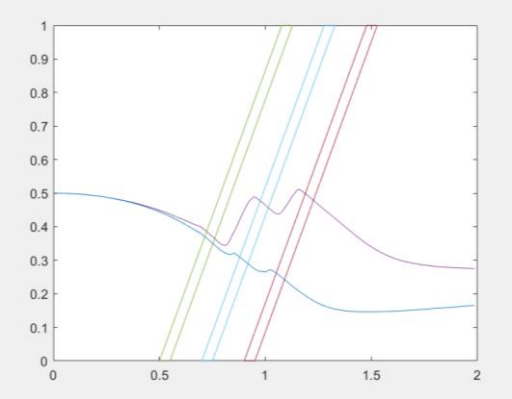

Figure 4. Proof-Of-Concept Particle Trajectory Simulation. X and Y axis represent the spatial axis of the device. Purple line is simulated to rise higher in Z axis than blue line. Colored polygons represent ridge regions.

CHAPTER 5

DISCUSSION

The results that can be seen in figure 3 were unexpected, and do not seem to be what was anticipated by authors who previously utilize similarly constructed devices (4, 5). Various authors in this field discuss the cells in these microfluidic devices as being sorted based on their exposure to two separate flow patterns. It has been discussed that cells with high stiffness will be influenced more by primary flow, while cells that are very soft or viscous will be influenced more by secondary flow (4,5). This binary classification may not be entirely accurate though. If this simulation is accurate, it would suggest that the extent to which secondary flow affects the overall trajectory is determined also by how much the cell will rise in-between ridges. The figure shows that the flow is always in the negative y direction in-between the ridges, at the height cells are at when they flow underneath the ridge. In other words, if the simulation is accurate, then the cells must be rising up in-between each ridge. A possible cellular property that could affect the amount that a cell rises would be cellular mass, or inertia. This claim can be backed up with experimental results as seen in an experiment performed by a group that had solid particles of various sizes flow through this device, with the goal of computationally estimating the z coordinate of a particle based on the on various image distortion characteristics that correlate with the particle's distance from the camera (14). In this experiment by Tasadduq et al., it was observed that smaller particles, which contain less mass and inertia than larger particles, would rise higher and be displaced more along the y axis in-between ridges. This result supports the claim that the height to

which particles rise in-between ridges will have a large effect on their lateral displacement in these sections.

In figure 4, a proof-of-concept simulation was conducted, where the only force on the particle was due to water. In this simulation, it was observed that a particle which rises more in-between two ridges, presumably due to having a lesser mass, will be displaced further in the positive y direction. This result is, based on how the simulation was set-up, due to the simulated flow field defining the regions with a greater z value as having a greater flow in the positive y direction. This figure demonstrates the importance of being able to track and simulate the displacement of a cell in the z direction, due to how this will determine the force it is experiencing in the y direction.

CHAPTER 6

CONCLUSIONS

In this paper, a flow simulation was conducted of microfluidic ridge devices that have previously proven successful in cell sorting. This simulation was conducted in OpenFOAM, using a mesh that was created in Gmsh. Based on the visualization of the resulting simulated flow field, it appears that the flow across the entire ridge section is in the negative y direction, at heights that are lesser than the gap underneath each ridge. Additionally, based on the proof-of-concept particle simulation, it seems likely that in order for cells to be displaced in the positive y direction in-between ridges, they must be rising in-between each ridge. These results provide a new understanding on how cell sorting occurs in this device design, as well as how the design parameters may be promoted in order to promote cell sorting.

In future studies, it is necessary to incorporate the force that is applied to the particles by the ridge into the simulation. One of the primary ways that cell sorting occurs in these devices is from the normal force that the wall exerts on the cell as it is squeezing beneath the ridges (4). Additionally, it will be important to have a video recording of the z coordinates of cells as they pass through this device. The current recordings we have do not contain information about the z coordinates, as this was not anticipated to be an influential detail. For a future useful cell trajectory simulator to be created, it must be able to account for the force of the ridge on cells, as well as the z position the cell is in at any point in time. If this can be done, it will be possible to simulate which flow chamber parameters will result in maximized lateral separation of cell types, which will result in

maximized cell sorting. An accurate cell trajectory simulator will bring this technology much closer to being a viable convenient and cost effective method for sorting cells.

REFERENCES

1. A.P. Phillips, K.L. Martin, Limitations of flow cytometry for the specific detection of bacteria in mixed populations, In Journal of Immunological Methods, Volume 106, Issue 1, 1988, Pages 109117, ISSN 0022-1759 2
2. Shields CW, Reyes CD, López GP. Microfluidic Cell Sorting: A Review of the Advances in the Separation of Cells from Debulking to Rare Cell Isolation. Lab on a chip. 2015;15(5):1230-1249. doi:10.1039/c4lc01246a.
3. Mark, D., et al. (2010). "Microfluidic lab-on-a-chip platforms: requirements, characteristics and applications." Chemical Society Reviews 39(3): 1153-1182.
4. Wang, G., et al. (2015). "Microfluidic cellular enrichment and separation through differences in viscoelastic deformation." Lab on a Chip 15(2): 532-540.
5. Wang, G., et al. (2015). "Cellular enrichment through microfluidic fractionation based on cell biomechanical properties." Microfluidics and Nanofluidics 19(4): 987-993.
6. Yang, X. N., et al. (2017). "High-throughput and label-free parasitemia quantification and stage differentiation for malaria-infected red blood cells." Biosensors & Bioelectronics 98: 408-414.
7. Jeong, J., Frohberg, N. J., Zhou, E., Sulchek, T., & Qiu, P. (2018). Accurately tracking single-cell movement trajectories in microfluidic cell sorting devices. *PloS one*, *13*(2), e0192463.
8. X. Hu, P. H. Bessette, J. Qian, C. D. Meinhart, P. S. Daugherty and H. T. Soh. “High purity microfluidic sorting and in situ inactivation of circulating tumor cells based on multifunctional magnetic composites” Proc. Natl. Acad. Sci. U. S. A., 2005, 102, 15757–15761
9. Geuzaine, C., & Remacle, J. F. (2009). Gmsh: A 3-D finite element mesh generator with built-in pre-and post-processing facilities. International journal for numerical methods in engineering, 79(11), 1309-1331.
10. Jasak, H., Jemcov, A., & Tukovic, Z. (2007, September). OpenFOAM: A C++ library for complex physics simulations. In International workshop on coupled methods in numerical dynamics (Vol. 1000, pp. 1-20). IUC Dubrovnik, Croatia.
11. Ahrens, J., Geveci, B., Law, C., Hansen, C., & Johnson, C. (2005). 36-paraview: An end-user tool for large-data visualization. The visualization handbook, 717.
12. Hughes, T. J., Cottrell, J. A., & Bazilevs, Y. (2005). Isogeometric analysis: CAD, finite elements, NURBS, exact geometry and mesh refinement. Computer methods in applied mechanics and engineering, 194(39-41), 4135-4195.
13. Courant, R., & Hilbert, D. (1965). Methods of mathematical physics [Methoden der mathematischen Physik, engl.] 1. CUP Archive.
14. Tasadduq, B., et al. (2015). Three-dimensional particle tracking in microfluidic channel flow using in and out of focus diffraction.